EQUATORIALLY TRAPPED PLASMA POPULATIONS

Richard Christopher Olsen

Physics Department, University of Alabama, Huntsville, Alabama, 35899

Abstract. Plasma observations made at $5.5R_E$. by the USCD detectors on the SCATHA satellite reveal the existence of a thermal plasma population trapped within a few degrees latitude of the magnetic equator, defined here as the minimum B surface. These measurements were restricted to the 1000 to 2000 LT sector by the spacecraft orbit. The ions show a higher degree of anisotropy than the electrons, with a FWHM of 10° to 25°, narrowing with increasing energy. The electron distribution shows a width of 20 ° to 60°, again narrowing with increasing energy. The 20- to 100-eV ion fluxes typically show temperatures in the 20- to 50-eV range, and densities of 1-10 cm^{-3}. The electron population typically extends from 50 to 500 eV, with temperatures of 100-200 eV and densities also in the 1- to 10-cm^{-3} range. Lower energy field-aligned populations are occasionally found in both ions and electrons at the same location. These could be sources for the warmer pancake plasma if heated primarily in the perpendicular direction. Equatorial noise in the 20- to 200-Hz range is seen in the electric field data about 90% of the time in association with the trapped plasma, with an intensity corresponding to the strength of the trapped fluxes.

Introduction

Plasma measurements have been made by a great variety of instruments at or near the earth's magnetic equator, and it is generally recognized to be a major reservoir for plasmas of all energies. Measurements made on GEOS 1 and 2 [Wrenn et al., 1979] indicate that low energy electrons (0-500 eV) are one such population, trapped at the equator, and much denser than the plasma mirroring away from the equator. Plasma measurements from the P78-2 (SCATHA) satellite, launched in 1979, showed the same electron population, and an even more severely trapped thermal ion population (10 to a few hundred eV). Two distinct wave phenomena complement these plasma measurements. Gurnett [1976] reports an electromagnetic wave in the 20- to 100-Hz range, which is strongly limited in its latitudinal extent. Wave data taken on SCATHA shows a strong correspondence between this type of wave activity and the trapped plasmas. A second wave phenomenon associated with the equator is an electrostatic wave in the 10-kHz range. Gough et al. [1979] report on the relationship between these $(n + 1/2)tce$ waves and the plasma measurements described by Wrenn et al. [1979] for GEOS.

The SCATHA observations of the equatorially trapped plasmas are presented here, with the intention of presenting a first look at the data, and reinforcing the importance of making measurements at the equator. The sections that follow describe the satellite and instruments, beginning with the UCSD plasma detector and the GSFC elec-

tric field experiment, and then briefly describing the pertinent characteristics of the magnetometer and mass spectrometers. Following the instrument descriptions, two events are described in detail. This is followed by a brief description of the general nature of the equatorial observations on SCATHA and the discussion.

Spacecraft and Instruments

The Air Force P78-2 (SCATHA) satellite was launched on January 30, 1979, reaching its final, near geosynchronous, orbit on February 7, 1979. The cylindrical spacecraft rotates at a relatively slow 1 rpm about an axis lying in the orbital plane and nominally perpendicular to the earth-sun line. Perigee was at 5.3 R_E, apogee at 7.8 RE, and the orbital plane was inclined by about 8°. The satellite drifts eastward about 5.1° a day, thus varying the local time for perigee and apogee. The inclination of the orbit and the radial variations combine to make the observation on this satellite considerably different from those on GEOS 1 and 2. The observations discussed here were made when the satellite was near perigee and crossing the equator, moving a few degrees in latitude in an hour. The GEOS 2 observation published by Wrenn et al. [1979] came from a period when the satellite was quite close to the magnetic equator for an extended time period, at 6.6 R_E. Wave observations by Gurnett came from IMP 6 (near equatorial, 26° inclination) and Hawkeye (polar orbit) inside 5 R_E.

The UCSD plasma detector is similar to the one flown on ATS 6, as reported by Mauk and Mcllwain (1975). The experiment consists of 5 electrostatic analyzers (ESA's), 3 for ions and 2 for electrons. Pairs of ion and electron ESA's are mounted in rotating heads, with the third ion detector mounted to look radially outwards. The rotating detectors sweep in orthogonal planes, sweeping through the spin axis and outwards radially. One of the rotating assemblies (HI detector) has an energy range of 1 eV to 81 keV, while the other rotating assembly (LO detector) and the single ion detector (FIX detector) cover the 1 eV to 1800 eV energy range. Energy resolution ($\Delta E/E$) is 20%, with adjacent channels generally overlapping in energy coverage. Both detectors cover a 64-step energy scan in 16 **S.** A frequently used option is to dwell for short time periods between energy scans at specific energy levels. These dwells can last from 2 to 128 s, thus providing excellent pitch angle coverage (as the spacecraft rotates) at some expense in energy coverage. The detector apertures have an angular pattern of about 5° x 7°, the narrow direction being perpendicular to the spin axis when looking radially outwards. The mode that provided most of the data for this study involved fixing one of the rotating heads parallel to the spin axis and the other perpendicular to it with dwells at several energies for periods of 15 to 60 s. This

provides good energy coverage of the equatorially mirroring (perpendicular to B) fluxes in the head parallel to the spin axis, and good angular coverage at a few energies in the detectors looking radially outward. The electron sensors have a strong sun response, but the ion detectors appear to be free of sun contamination. One additional mode selection of note in this data is the option of suppressing the low energy electrons. Electrons below 30 eV in the HI detector, and 10 eV in the LO detector can be suppressed to avoid counting photoelectrons. This option also affects the background rate below 100 and 26 eV, respectively.

The GSFC electric field detector is a double floating probe, with 100 m (tip to tip) antenna extending radially from the spacecraft. It is designed to measure electric fields from DC up to 200 Hz. The data used for this study were from a pass band filter output covering the 20 to 200 Hz frequency range. In this range, the detector has a minimum sensitivity of about 50P Vim.

The GSFC magnetic field monitor provides the data necessary to determine pitch angles, and a wave output to the electric field spectrometer. Unfortunately, the magnetometer has a threshold of about 100 milligamma in the 20- to 200-Hz range, well above the 20 milligamma amplitude for the equatorial noise reported by Gurnett.

Data from two mass spectrometers were also examined. The MSFC light ion mass spectrometer (LIMS) was designed to cover the 0- to 100-eV range, while the Lockheed energetic ion composition experiment (ICE) was built to measure the 100-eV to 32-keV population. The LIMS unfortunately failed prior to the best equatorial events, but does provide some information on a probable early case. The Lockheed instrument has been previously described in some detail [Kaye et al., 1981]. The detectors have an angular resolution of 5° FWHM and energy resolution of 10%. In the low mass range, the instrument covers the 0.8- to 80- AMU range. The data of interest come from a detector that measures 100- to 580-eV fluxes. These data are useful but do not cover the normal energy range of the peak ion flux. The geometric factor for this instrument is substantially lower than that of the UCSD detector, and substantially fewer counts are measured in the short accumulation interval. This introduces a moderate problem of statistical fluctuations in the data for the events to be present-ed.

Observations

Since the equatorial fluxes are frequently several orders of magnitude higher than those a few degrees off the equator, locating the trapped plasma population in survey spectrograms was not difficult. The magnetic equator is defined here as the minimum B surface, the location defined by the trapped plasma. The magnetic dipole latitude was found to not always be a reliable guide to the equator, and regions several degrees away in latitude were included in the survey. In six months of operation, about fifty equator crossings were identified, with the presence of trapped plasma and wave activity indicating the satellite had actually reached the equator. The two events presented below were selected for

their relatively high fluxes, and in the first case, the clear correspondence between wave and plasma, but are not otherwise anomalous.

Day 136

The first case to be presented is a good example of both the trapped plasma and wave activity. The plasma detector was arranged so the high-energy head (HI) was parked parallel to the spin axis, and the low energy rotating detector (LO) was parked looking almost radially. The observation comes at local dusk, at about 5.5 R_E. In this mode, at this local time, the HI detector is looking east, while the other two detectors view the earth-sun line when at 90° pitch angle. The keV electron data seem to indicate that the satellite is earthward of the plasma sheet, in the bulge region of the plasmasphere or in the plasma trough between the plasma sheet inner boundary and the plasmapause. Figure 1 shows the flux and electric field wave measurements as the spacecraft approaches and crosses the magnetic equator. The 78 and 233 eV ion fluxes are plotted in the top portion of the figure, the electric field data are plotted at the bottom. Plasma data are taken at 90° pitch angle, as the dwell pattern of the energy coverage intersected the rotation through the 90° plane. The fluxes increase rapidly as the spacecraft comes within 2° latitude of the equator, while the electric field data shows a remarkably smooth variation with latitude. The wave is linearly polarized, with the electric component perpendicular to the magnetic field line, and the magnetic perturbation is parallel to the field line. This polarization shows in the modulation of the wave amplitude with the spacecraft spin period.

The idea that there is a dense plasma trapped at the equator is verified by a look at the pitch angle distribution of the ions near the peak in flux at 1815 UT (Figure 2). Data from the FIX detector energy dwells are plotted as function of pitch angle for 8.4, 26.3, 78.5, and 233.4 eV. The high degree of anisotropy of the ion population is apparent here, with the anisotropy increasing with energy. The widths of the distributions (FWHM) are 27° at 8.4 eV, 20° at 26.3 eV, 12° at 78 eV, and about 8° at 233 eV. Data points from the fixed detector represent 0.125 s accumulations, which correspond to a 0.8° rotation of the spacecraft. Increasing pitch angle means the detector is looking toward the sun at 90°, while decreasing pitch angle indicates the detector is looking tailward.

The electron pitch angle distributions required several 15-s dwells to fill the 140° range shown in Figure 3. The electrons are not nearly as anisotropic as the ions, particularly at low energies, but the same effect is found here in data from the LO detector. A strong central peak (FWHM=30°) is evident in the 233 eV data looking tailward, with a broader distribution at 78 eV (FWHM=65°). Data from the sun sector have been omitted. The detector look direction comes within about 25° of the magnetic field line, and a distinct loss cone is just appearing at that point. One peculiarity is the conic, which appears at 1809 UT, but not at 1812. The 233 eV electron flux shows a local maximum at 154°, dropping quickly again at 156° .   This feature
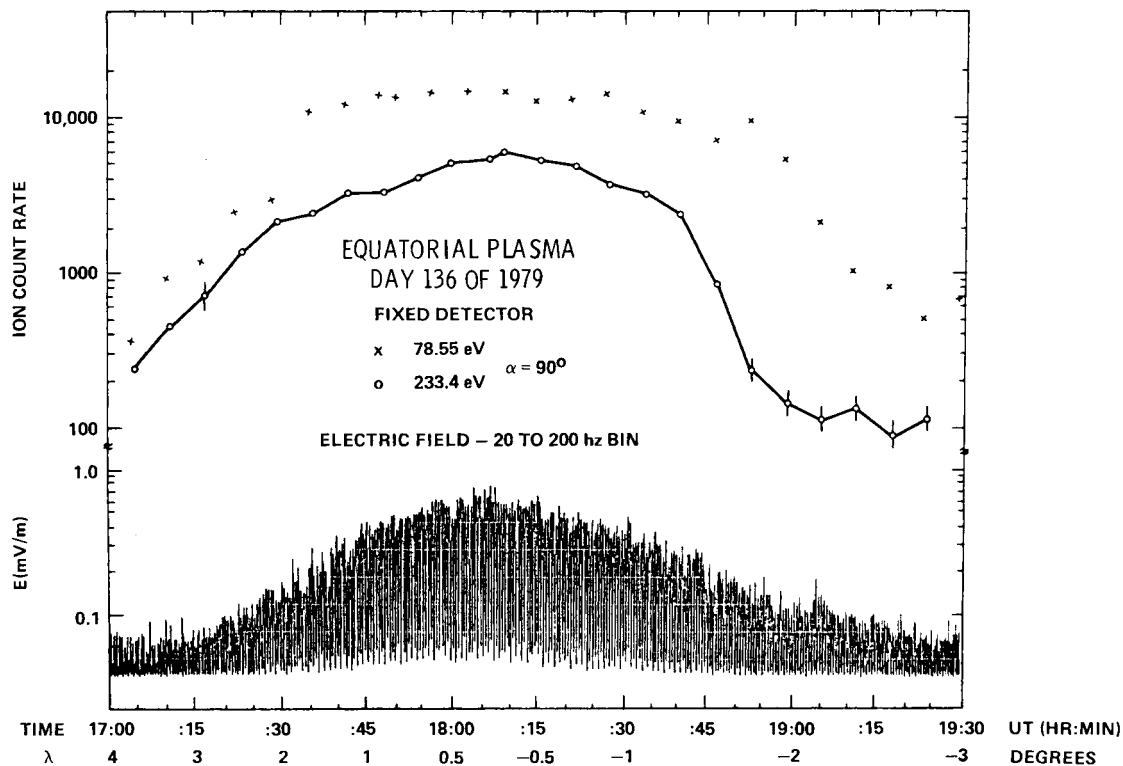
Fig. 1. Plasma and wave variations with latitude for day 136 of 1979. The 78 and 233 eV ion fluxes at a =90° are shown here along with the electric field output from the 20-200 Hz pass band filter. The electric field output is modulated by the spin frequency of the spacecraft, since the wave is polarized.

appears in other dwells in this time period and appears to be real (i.e., not a time dependence). The ion data show poor statistics at low pitch angles, but a mild loss cone is visible there as well. The second example will display the field-aligned plasma behavior more clearly. At the equator, the ion fluxes drop to the level of the isotropic background at about 500 eV, the electrons at about 1 keV.

The 78 eV ion fluxes are near the peak in the count rate versus energy scan at the equator (a fortunate coincidence) and they are used here to study the variation in the pitch angle distribution away from the equator. Figure 4 shows the intensity dropping and the distribution widening as the spacecraft moves away from the equator. Simple field line mapping shows that the equatorial flux distribution found at 1728 maps to the distribution found at 1815 for a shift of 4° latitude. The change in magnetic dipole latitude here is only 2.6°, so there are apparently also some mild spatial or temporal variations in the plasma density over the 45-m interval. A search for asymmetries in the sun-tail direction was inconclusive, partly because of the detector mode, but it appears that such effects are absent on this day.

Figure 5 shows the ion distribution functions at and near the equator, as measured by the HI detector. At the equator this detector measures the 90° pitch angle population, and these measurements agree with those made by the FIX detector.   The observed pitch angle changes with

latitude since the detector is parked along the spin axis. Since the degree of anisotropy increases with energy, the higher energy (100 eV < E < 1 keV) trapped plasma is not being sampled away from the equator. The distribution at the equator is unremarkable, showing no obvious breaks or peaks.

The distribution functions were least square fitted with Maxwellians to provide estimates of the density and temperature. The density resulting from such a fit is real only for an isotropic environment and so is denoted $4\pi\partial/\partial\Omega$. An estimate of the actual density (averaged over pitch angle) can be obtained by dividing by 5 for the ions. The result for fitting the equatorial distribution function shown in Figure 5 between 25 eV and 100 eV is a temperature of 34 eV and density ($4\pi\partial/\partial\Omega$) of 39 cm^{-3}. The 100- to 300-eV ions show a temperature of 53 eV and a density of 28 cm^{-3}.

The low energy (2-25 eV) ion fluxes obtained from the fixed detector energy scans near 90° pitch angle show relatively poor statistics (hundreds of counts) and are strongly affected by the spacecraft spin during the energy scan period. Most of the scans occurred while looking tailward. With these limitations noted, the distribution seems to flatten below 20 eV, with a hint of a cold (1 eV) population superimposed.

The electron distribution function is shown in Figure 6, with two energy scales to display the straight-line (Maxwellian) nature of the population over the 25- to 200-eV range. The electron
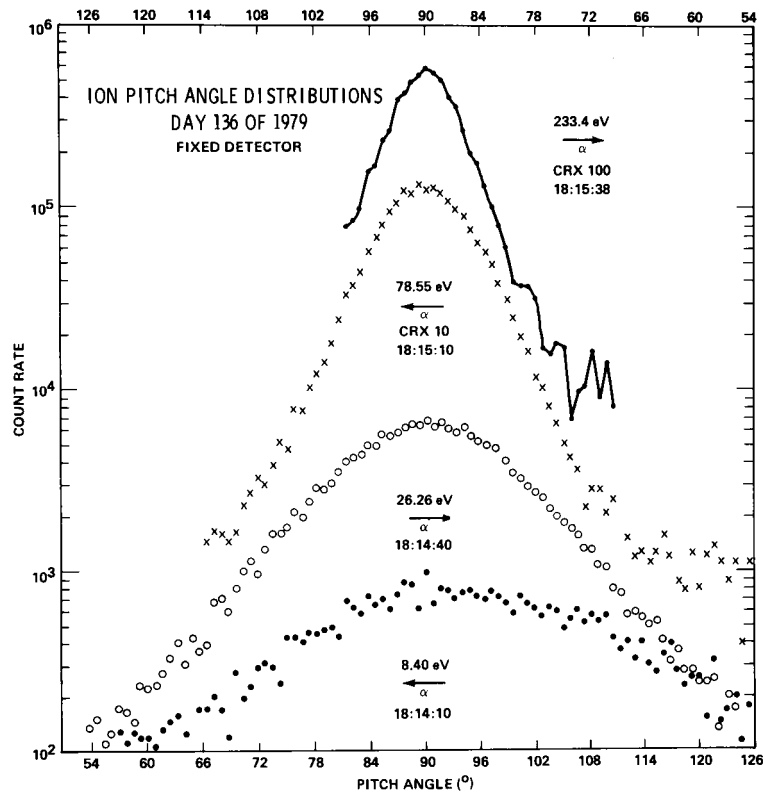
Fig. 2. Ion pitch angle distributions for the equatorial plasma on day 136 of 1979. Data are presented at 8.4, 26.3, 78, and 233 eV. Data points are taken every 0.125 s in the FIX detector, or about 1° of rotation. Increasing pitch angle (arrow towards right) is associated with tailward ion motion (looking towards sun), decreasing pitch angle with sunward motion.

data below 25 eV are disturbed by locally gene-rated photoelectrons and a detector dependent problem unique to the HI detector. The fit in the 50- to 150-eV range gives a temperature of 54 eV and a density of 3.0 cm^{-3}, while the 165- to 450-eV data give a temperature of 118 eV and a density of 2.3 cm^{-3}. The difference in ion and electron densities would presumably drop if the entire phase space were included in the density determination.

The mass spectrometer data in the 100- to 500-eV range show a fair agreement with the UCSD data, in terms of the measured flux, and the additional information that about 90% of the fluxes in that energy range are hydrogen. It is important to note that the lower energy fluxes could have an entirely different mass composition.

A comparison between the magnetic field data and a model field show a fair agreement, which is reasonable for a quiet period like this, and we conclude this section by noting that the magnetic dipole latitude is probably valid for this case.

Day 179

The second major example came in the next series of equator crossings, on day 179 of 1979. The detector mode is considerably different on this day, both in orientation and energy cover-age. The LO detector is parked parallel to the spin axis, while the HI detector is looking radially outward. The detector was set for 60-s dwells, and the combination of the HI and FIX detectors looking radially gives excellent pitch angle distributions for ions at 5 useful energies from 11 to 900 eV. Figure 7 shows the pitch angle distribution found for the ions at the equator. A full 360° pitch angle range is provided here, with the detector measuring to within 3° of the field line (0° is in the detector field of view). The spacecraft is near 5.5 RE with the equator crossing at about 1000 LT. The LO detector is therefore looking west. The radial detectors again view near the earth-sun line. The plotting convention here is that pitch angles greater than 180° correspond to looking earthward
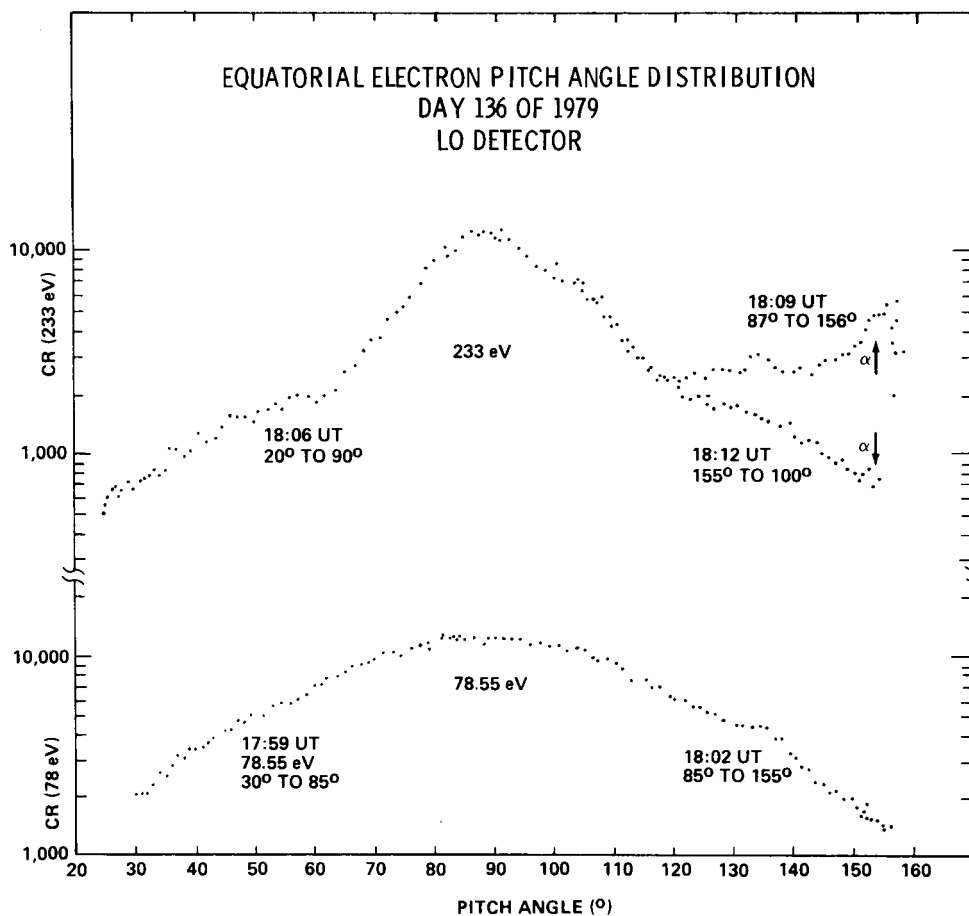
Fig. 3. *Electron pitch angle distributions on day 136 of 1979, at 78 and 233 eV. Data points are from 0.25-s accumulations and correspond to 1.6° of spacecraft rotation. Two dwell periods were used to construct the 78 eV distribution, with three used at 233 eV.*

(ion motion is towards sun). The trapped fluxes are clearly visible from 11 to 523 eV, and suggested at 900 eV. The distribution again narrows with increasing energy, and peaks between the 40 and 100 eV distributions shown here. The widths of the distributions (FWHM) are, in increasing energy, 25°, 12 °, 9°, and 60° -70° at 900 eV. A new feature here is the sharp loss cone visible in the 103, 523, and 900 eV populations. Conical distributions are visible around the loss cone, in particular at 523 eV. A distinct peak is found at 160°/200° pitch angle, with a width of 15° to 20°. At the minimum, the 523 eV channel gives a count rate of 40 c/s, rising to 200 c/s at 25°, dropping down to 100 c/s at 50° to 60°, then rising to 500 c/s at 90°. There is a persistent difference in the two maxima at most energies, with the earthward fluxes averaging a few percent higher than the sunward fluxes. This does not appear to be a flow, since it does not favor low energies.

The electron data, shown in Figure 8, display a similar behavior, with one intriguing addition. Electron fluxes at 41, 523, and 4730 eV are plotted for the sector that is not contaminated by the sun pulse. The 523-eV fluxes are near the peak of the trapped electron distribution and show a pitch angle distribution similar to that found on day 136.

The 523-eV peak has a width of 19°, which is relatively narrow for the trapped electron populations measured in this study. There is a sharp loss cone, 15° to 20° wide superimposed on the broader distribution. The 4730-eV fluxes show a similar behavior. The new feature shown in Figure 8 is the source cone, or field-aligned, electron flux at 41 eV. This distribution shows no evidence of being a conic, as in the ion distributions. The combination of a high-energy pancake/loss cone distribution and a low-energy source cone distribution suggest that both the input and output of a heating process are in view here, and it is interesting to consider the possibility of an ion source as well.

The trapped ion population consistently shows a lower energy than the electron population (by a factor of 5 to 10), and it seems reasonable to look for the field-aligned ion population at a few eV. The lowest energy ion dwell, at 11 eV, has been shown in Figure 7, and these fluxes do not show a source cone or a loss cone. The next possibility for locating field aligned ions is in the energy scan data. There is such a scan in the FIX detector at 2136 UT (just prior to the 41-eV electron dwell data) as the detector rotates through the 1° to 15° pitch angle range, and there is indeed such a field-aligned ion
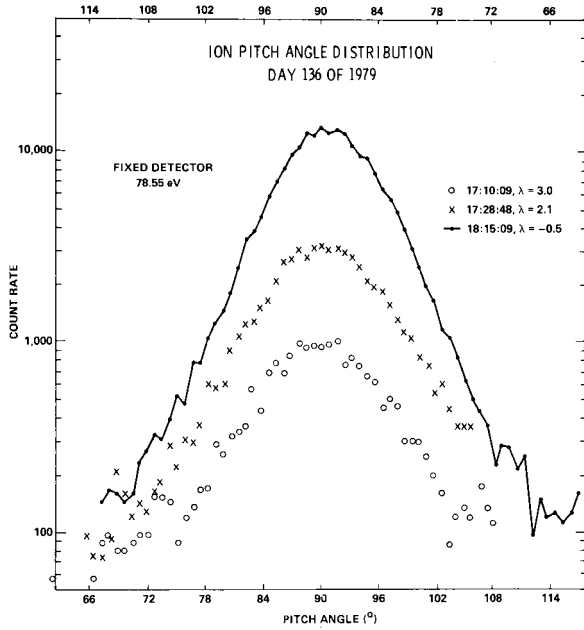
Fig. 4. Ion pitch angle distributions at and near the equator at 78 eV, day 136 of 1979. Latitudes are from a magnetic dipole model.
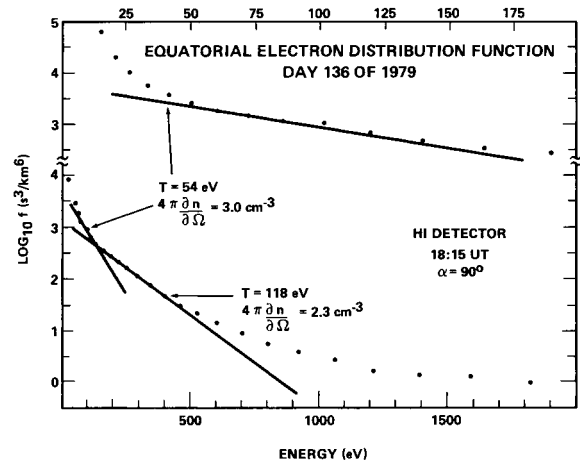

Fig. 6. Electron distribution functions at the equator, day 136 of 1979. The energy scales are split with low-energy fluxes and scale plotted at the top and higher energy fluxes plotted below with a scale on the bottom axis. This detector is not well calibrated below 25 eV. at 30° and remaining at that level out to 90°. (The 2.4 eV dwells on day 136 show no apparent source cone for ions).

population, peaking in count rate at 2.8 eV. The pitch angle distribution of the 2.8 eV ions was examined, and though the coverage is poor, there is a clear maximum along the field line, dropping rapidly from 200-300 c/s at the peak to 100 c/s

The energy distributions of the trapped and field-aligned fluxes are shown in Figures 9-11. The electron count rate and distribution function are shown for $90°$ pitch angle in Figures 9 and
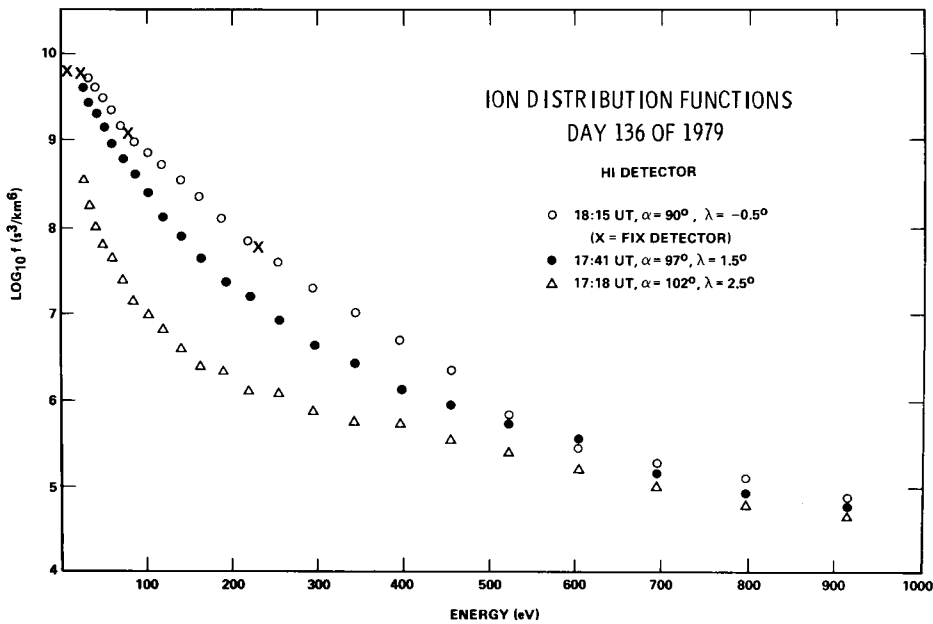

Fig. 5. Ion distribution functions at and near the equator from the HI detector, day 136 of 1979. Pitch angle varies with latitude because the detector is fixed looking along the spin axis of the satellite.
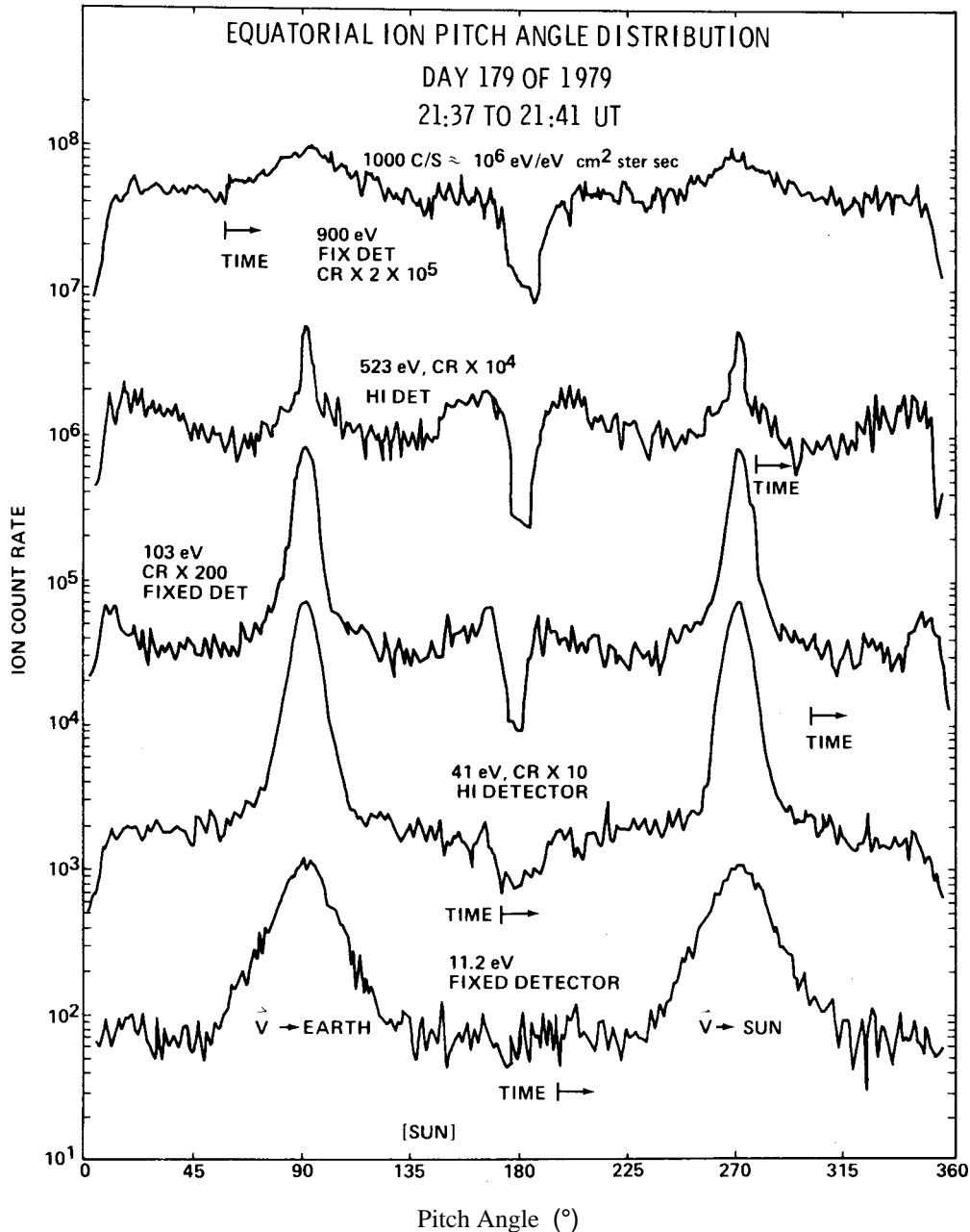
Fig. 7. Ion pitch angle distributions at the equator for day 179 of 1979. Data are plotted from the FIX and HI detectors at 11, 41, 193, 523, and 900 eV. Fluxes are scaled by increasing factors to keep them from overlapping. Maximum values, with increasing energy are 1150 cis, 7300 c/s, 4200 c/s, 550 cis, and 540 c/s. The 0°-180° range corresponds to looking sunward, with 0° corresponding to looking south.

10, respectively. The count rate peaks in the 500- to 1000 eV region but is not particularly Maxwellian. A fit to the 100- to 1000-eV electron data gives a temperature of 250 eV and a density of 2.4 cm^{-3}. The field-aligned electrons (not shown) have a temperature of 10 eV in the 30-70 eV range, and a density of 5 cm^3.

The ion distributions measured by the LO and FIX detectors are shown in Figures 9-11. The ion sensor of the LO detector has dropped in overall sensitivity at this time, and a difference in flux is apparent between the LO and FIX ion data in Figure 9. Dwell data was taken from the FIX detector at 90° pitch angle, and the trace of the LO energy scan

superimposed. The match at the 3 energy levels suggests that the spiraltron de-gradation in the ion detector has not introduced any energy dependent changes in the detector sensitivity. (The LO detector electron spiraltron does not appear to have degraded at this bias level). The ion count rate peaks at about 50 eV, and the fit to the trapped ion distribution function shown in Figure 10 in the 25- to 100-eV range gives a temperature of 25 eV. The fitted density (uncorrected for spiraltron decay) is 7.1 cm^{-3}. The temperature in the 100- to 350-eV range is 60 eV. The inset graph in Figure 10 shows the low-energy portion of the ion distri-
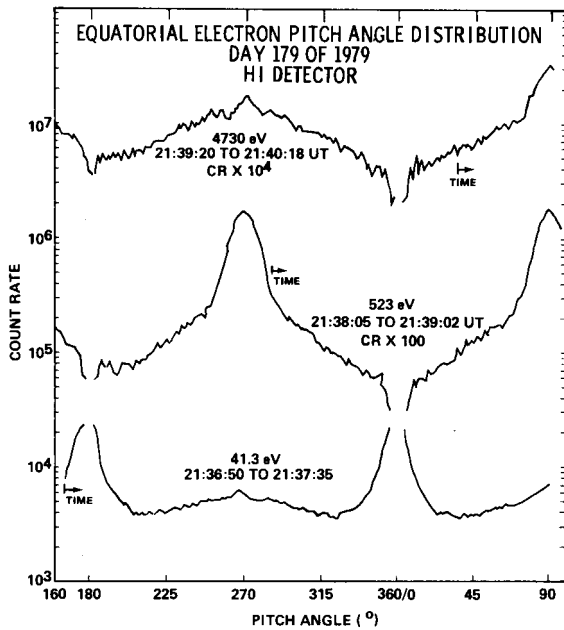
Fig. 8. Electron pitch angle distributions at the equator for day 179 of 1979. Data are plotted from the HI detector at 41, 523, and 4730 eV. Pitch angle conventions are as in Figure 7.
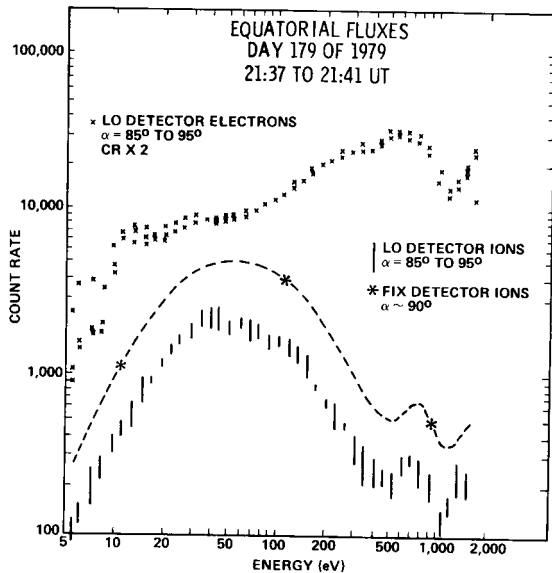

Fig. 9. Ion and electron count rates as a function of energy from the LO detector near 90° pitch angle for day 179 of 1979. The electron count rate has been scaled by a factor of 2. The count rates from the FIX detector dwells were selected at their maxima (90° pitch angle). The difference between the LO and FIX ion data reflects degradation of' the spiraltrons for the LO ion detector. The LO count rate curve has been traced and moved up to overlap the FIX detector data (about a factor of 2). The peak in ion count rate at 700 eV is a local maximum in the distribution function as well (see Figure 10).
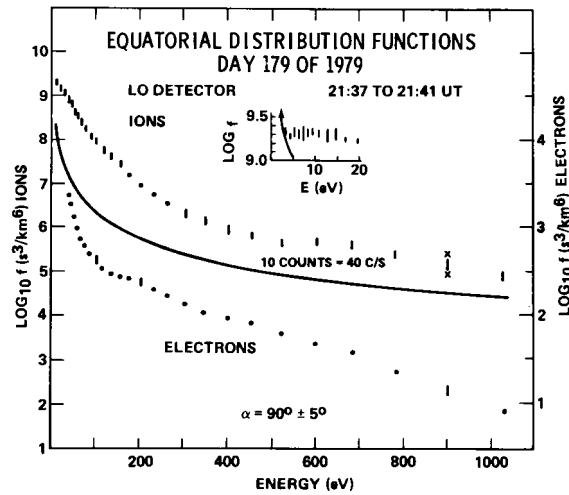

Fig. 10. Ion and electron distribution functions from the LO detector for day 179 of 1979. The data shown in Figure 9 are replotted here. The ion data have not been corrected for spiraltron degradation. The top curve is the ion plot, with the solid line below showing the background level, a conservative 10 count/accumulation, or 40 c/s. The low-energy ion data are shown in the inset plot, again with a 40 c/s background indicated. The 11-eV data point in the inset plot is from the dwell data. The lower, dotted plot shows the electron data. The local maximum at 700 eV was originally noticed by J. Fennell in the data set from his detector on SCATHA.

bution, which appears to flatten out, indicating either a flow or a significantly nonthermal character to the plasma. The latter case appears more likely, given the shape of the curve.

Figure 11 shows the field-aligned ion distribution function as measured by the FIX detector when it rotated through the field line. This is a plot of the flux which peaked in count rate at
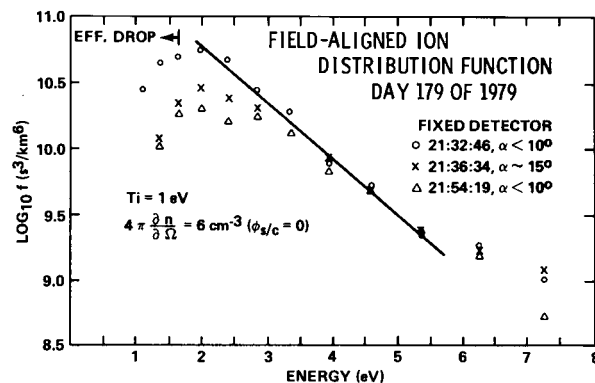

Fig. 11. Ion distribution function for field-aligned ions, day 179 of 1979. Data from the FIX detector were selected for pitch angles less than 15 °. The 2-to 5-eV data have been least square fitted, with the result drawn through the data points. There is a detector efficiency drop (EFF. DROP) below 2 eV causing the decrease in the distribution function below that point

2.8 eV, now fitted with a 1 eV Maxwellian in the 2- to 5-eV range. An additional detector dependent effect appears in this data that has not been apparent in the distribution function plots. The detector efficiency has a distinct drop below 2 eV, which is apparent at all times in both the LO ion and electron data and the FIX ion data. This is attributed to variations in the contact potential along the ESA's, and to a lesser degree, variations in the plate voltages. Also, the spacecraft potential, ignored until now, be-comes an important consideration when trying to measure particles with an energy of a few eV. A lack of electron data below 10 eV makes it difficult to estimate the potential, but data from other time periods and the existence of ion flux-es in the 2- to 6-eV range suggest that the potential is on the order of +2 V. With this in mind, the result of the Maxwellian fit was a density (4n a n/aS2) of 6 cm^{-3}, assuming zero spacecraft potential. The estimated +2-V potential raises the fitted density to 44 cm^{-3} with a likely error of a factor of 2 either way (20-100 cm-3). Again, the narrow solid angle filled by the distribution means its contribution to the total density is small, from 2 to 10 cm^{-3}.

The last plot from this data set is Figure 12, a look at the variation in the ion and electron fluxes with latitude, along with the electric field data. The 523-eV electrons vary slowly over the 2.25-hour period, reflecting the relatively weak pitch angle anisotropy of the electron population. Both the 41 and 103-eV ion fluxes show a strong peak within a few degrees latitude of the equator. The wave data, however, do not show the smooth variation found on day 136, but rather show the wave ending abruptly at. 2125 UT. It appears from this plot that the wave-plasma correspondence is not as exact as Figure 1 implied initially.

The mass spectrometer data also show a differ-ence on this day. The statistics are again a problem, but the indication is that there is a relatively large flux of singly charged oxygen above 100 eV, and there is even the possibility that the oxygen density is comparable to the hy-drogen density.

General Observations

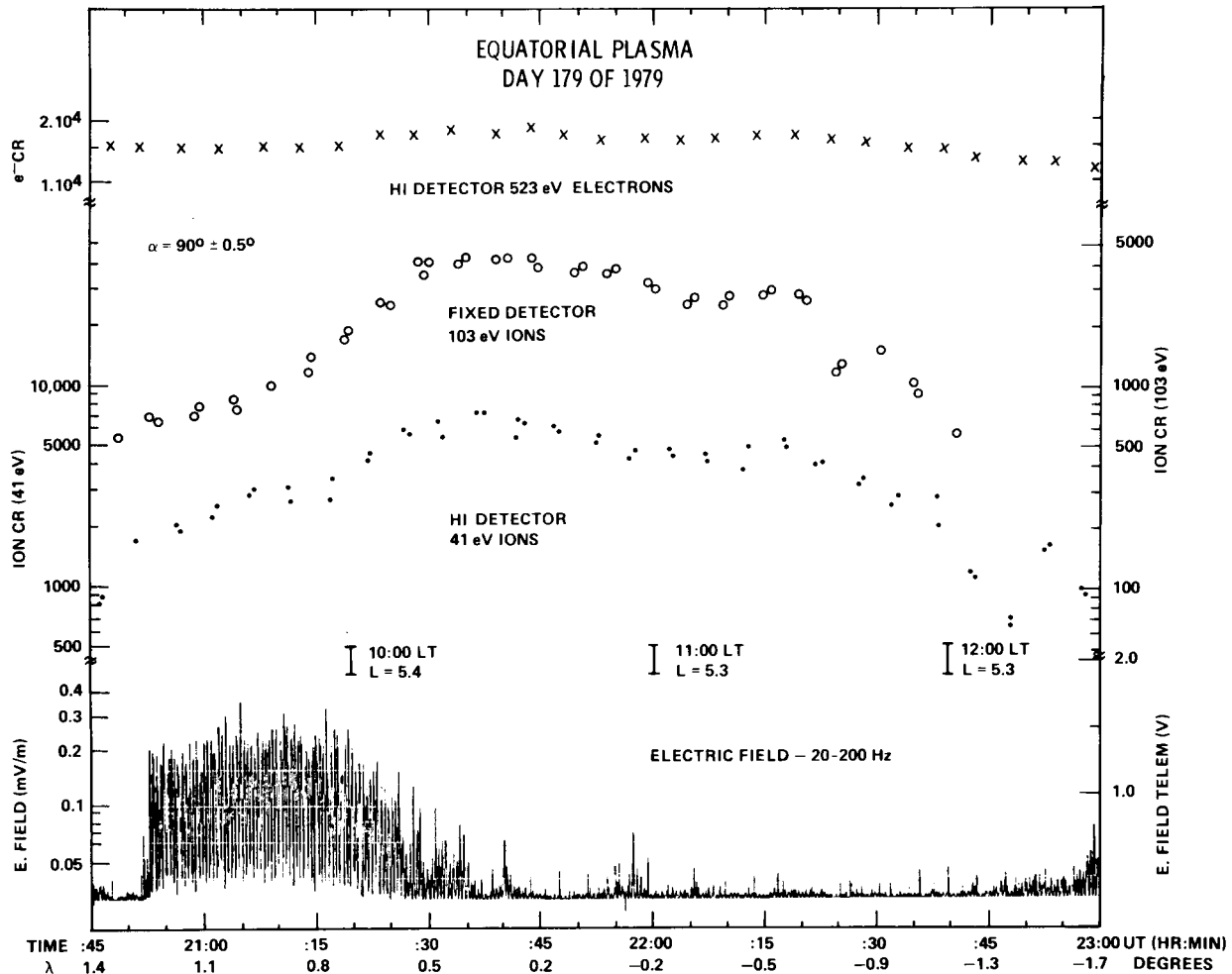The two events presented here are typical of the quiet time data acquired at the equator. The

Fig. 12. Plasma and wave variations with latitude for day 179 of 1979. The 41 and 103-eV ion fluxes and 523-eV electron fluxes at a=90° are shown here along with the electric field output from the 20-200 Hz pass band filter. Note that each of the three flux plots has a different vertical scale, but all are logarithmic.

magnetic activity index Kp was 0^+ for 1500-1800 on day 136, and 6- for the day. On day 179, the 1800-2100 value was 0^+, the 2100-2400 value was 1', and the sum for the day was 6. Most clear observations coincided with an absence of magnetic activity, but quiet periods did not always produce the population. The plasmas were variable over periods of a day (the observation interval). For example, the equatorial plasma fluxes were high on days 136 and 138, but weak on days 135 and 137, all quiet days. The trapped population was clearly present for several days following day 179, however, at local noon.

The equatorial noise signature in the 20- to 200-Hz filter data corresponded quite clearly to the presence of the trapped plasma. Twenty-nine cases of equator crossings were compared for the two data sets. In seventeen cases of 'strong' wave signatures (E> 0.2 mV/m), the clear correspondence with high plasma fluxes illustrated in Figure 1 was found thirteen times. Three of the other four cases showed relatively weak trapped fluxes, with the trapped component barely elevated over the isotropic background. The fourth case was the example shown in Figure 12 for day 179, where the wave and plasma signatures were offset in time. The twelve 'weak' wave events occurred at the same time as the plasma events in ten cases, with nine of these corresponding to weak plasma fluxes, and one to an event with high flux.

The mass composition in the 100- to 500-eV range was primarily hydrogen in the first event described here, while the second event may have been relatively rich in oxygen. An early observation of fairly weak fluxes on day 41 of 1979 coincided with the operational period of the low energy (0—100 eV) mass spectrometer. This observation showed the plasma to be primarily composed of hydrogen, with about 5% helium. Other studies of mass composition near the equator [Horwitz et al., 1981] showed that the 0-100-eV pancake distributions found near the equator were composed primarily of hydrogen, with some helium, but no oxygen. These distributions were found both inside and outside the plasmasphere. The ISEE 1 instrument used for these observations has a relatively wide aperture, and the spacecraft has a highly inclined elliptical orbit, which makes direct comparison with the SCATHA data difficult, but it appears that the same population is being reported by Horwitz et al.

This data set does not lend itself to an analysis of the local time dependence of the trapped plasmas, since the equatorial crossings in the observational period studied were grouped in the 0900-2200 LT region at low altitudes (R < 6.5 RE), and 0000-0900 outside 7 RE. Only one likely event was found in the equator crossings outside 7 R_E. The dawn to dusk events were relatively evenly distributed in that range, with a 30-50% chance of encountering the trapped plasma (and wave) on a given day. Most of the events were near dusk or noon, reflecting the satellite position during the two best sequences of equator crossings. The GEOS 2 observations of the trapped electrons were primarily in the dawn to noon sector, outside the plasmapause, in the plasma trough region. The two data sets are roughly complementary and suggest that the trapped plasma

population exists throughout the dayside, and continues past dusk. The continued existence of the thermal plasma on the nightside is likely and needs to be checked at 4 or 5 RE.

Discussion

The first thing the trapped population provides (when observed) is a marker for the earth's magnetic equator, defined as the minimum B surface. This would be particularly useful during active times, when the trapped population survives such activity. One such observation showed the trapped population at a dipole magnetic latitude of 5° at 1500 LT. These observations also indicated the dangers of inferring equatorial behavior and characteristics with measurements made more than a few degrees from the equator, and reinforces the idea that unique phenomena are occurring within a few degrees latitude of the minimum B surface defined by the trapped plasmas.

The challenge presented by these observations is an interesting one. If the initial source for this population is the ionosphere or plasmasphere, how was the plasma energized? If the plasma sheet is the source, where did the relatively high density come from?

Assuming a plasmaspheric source (cold and isotropic), perpendicular acceleration by a ion cyclotron wave would provide both the necessary energy and desired pitch angle distribution. This idea is supported by the increase in anisotropy of both species with increasing energy. The ion data for day 136, for example, could be fitted with a bi-Maxwellian distribution with a perpendicular temperature of 35 eV, and a parallel temperature of 1 eV. The ion pitch angle distribution found on day 179 can be roughly reproduced by a 50 eV perpendicular temperature and a 1 or 2 eV parallel temperature, roughly the values obtained in fitting the energy distributions. The electromagnetic wave seen at the equator by Gurnett [1976] and indicated here in Figures 1 and 12 has features which suggest structure at ion cyclotron frequencies (or harmonics). Curtis and Wu [1979] developed a theory suggesting that the wave obtains energy from the MeV particle population, and Curtis [1981] has suggested that the wave observed in conjunction with the trapped thermal plasma is indeed energizing it. It is possible, of course, that the trapped plasma is creating the wave activity or that the trapped plasma, field-aligned plasma, and 100-Hz wave activity are largely independent.

A plasma sheet source for these fluxes has problems with the pitch angle distribution, unless perpendicular acceleration is again invoked. Simple drift models [Chen, 1970] seem to indicate that the trapped fluxes are in regions of corotation. If this is ignored for the moment and a large cross-tail field is assumed to be driving the plasma inward, simple particle tracking shows that the typical field-aligned plasma sheet fluxes never become anything like the pancake distributions reported here in either energy or pitch angle distributions.

The substantial differences in the anisotropies of the ions and electrons raises an interesting question. If the difference in anisotropy

remains after integrating over all energies, there will be a net charge imbalance at some point along the field and thus a parallel electric field. It is not clear which might be causal.

Important questions that remain unanswered are the local time and radial dependence of the trapped plasmas, their dependence on magnetic activity, and the quantitative relationship between the waves and plasmas seen at the equator. These topics may be addressed with the data from the polar orbiting Dynamics Explorer satellite in the near future.

References

Chen, A. J., Penetration of low-energy protons deep into the magnetosphere, J. Geophys. Res., 75, 2458-2467, 1970.

Curtis, S. A., Equatorially trapped plasmasphere ion distributions and transverse stochastic acceleration (abstract), Trans. AGU, 62, 365, 1981.

Curtis, S. A., and C. S. Wu, Gyroharmonic emissions induced by energetic ions in the equatorial plasmasphere, J. Geophys. Res., 84, 2597-2607, 1979.

Gough, M. P., P. J. Christiansen, G. Martelli, and E. J. Gershuny, Interaction of electrostatic waves with warm electrons at the geomagnetic equator, Nature, 279, 515-517, 1979.

Gurnett, D. A., Plasma wave interactions with energetic ions near the magnetic equator, J. Geophys. Res., 81, 2765-2770, 1976.

Horwitz, J. L., C. R. Baugher, C. R. Chappell, E. G. Shelley, and D. T. Young, Pancake pitch angle distributions in warm ions observed with ISEE 1, J. Geophys. Res., 86, 3311-3320, 1981.

Kaye, S. M., R. G. Johnson, R. D. Sharp and E. G. Shelley, Observations of transient H~ and 0^+ bursts in the equatorial magnetosphere, J. Geophys. Res., 86, 1335, 1981.

Mauk, B., and C. E. Mcllwain, ATS-6 UCSD Auroral particles experiment, IEEE Trans. Aerosp. Electron. Sys., AES-11, 1125-1130, 1975.

Wrenn, G. L., J. F. E. Johnson, and J. J. Sojka, Stable 'pancake' distributions of low energy electrons in the plasma trough, Nature, 279, 512-514, 1979.